telecom

MDPI

Article

Stochastic Modeling of Mode Coupling and Steady-State Performance in Multimode Plastic Optical Fibers for Telecom Applications

Svetislav Savović [1,*], Matija Savović [2] and Xiong Deng [3]

[1] Faculty of Science, University of Kragujevac, R. Domanovića 12, 34000 Kragujevac, Serbia
[2] Faculty of Medical Sciences, University of Kragujevac, Svetozara Markovića 69, 34000 Kragujevac, Serbia; msavovic@uni.kg.ac.rs
[3] School of Information Science and Technology, Southwest Jiaotong University, Chengdu 610031, China; xiongdeng@swjtu.edu.cn
* Correspondence: savovic@kg.ac.rs

Abstract

Mode coupling in multimode step-index polymer optical fibers (SI POFs) plays a critical role in determining signal integrity and bandwidth performance in optical communication systems. It originates from intrinsic random perturbations that influence power distribution among propagating modes, making accurate prediction of steady-state distributions (SSDs) essential for reliable system design. In this work, we model mode coupling as a stochastic process using the Langevin equation, incorporating simulated Langevin forces to numerically evaluate modal power evolution and steady-state behavior. The proposed approach demonstrates strong agreement with previously reported experimental results, validating its capability to capture energy redistribution mechanisms induced by fiber imperfections. From a telecommunications perspective, the model provides valuable insights into modal dispersion, bandwidth limitations, and signal degradation in SI POF-based links. These results establish a robust and efficient framework for analyzing and optimizing multimode SI POFs, supporting their application in high-speed data transmission and short-reach optical communication networks.

Keywords: polymer optical fibers; telecommunications; Langevin equation; mode coupling; steady-state distribution

Check for updates

Academic Editors: Pierpaolo Boffi and Sotirios K. Goudos

Received: 6 April 2026
Revised: 12 May 2026
Accepted: 26 May 2026
Published: 29 May 2026

Copyright: © 2026 by the authors. Licensee MDPI, Basel, Switzerland. This article is an open access article distributed under the terms and conditions of the Creative Commons Attribution (CC BY) license.

1. Introduction

For decades, silica optical fibers have been the dominant transmission medium in long-distance communication systems [1,2]. In contrast, multimode plastic optical fibers (POFs) are widely considered for high-performance short-range links, typically below 100 m [3,4]. Owing to their large core diameter and high numerical aperture (NA), POFs enable efficient light coupling, making them attractive for applications such as power delivery [5,6], sensing [7,8], and short-distance communication systems [9,10]. Furthermore, POF technology shows significant potential for expansion in large-scale and complex infrastructures, mobile platforms, and environments where network reconfiguration is frequently required [11,12].

Mode coupling in optical fibers arises from intrinsic random perturbations, including microbending, impurities and compositional inhomogeneities, irregularities at the core–cladding interface, and local variations in the refractive index profile. POFs, typically

fabricated from materials such as polymethyl methacrylate (PMMA), exhibit optical properties that are strongly governed by their chemical structure. The carbon-based molecular backbone, particularly the presence of C–H bonds, leads to intrinsic absorption losses, most notably in the near-infrared spectral region. Optical performance is further influenced by the chemical purity of the material, as impurities and compositional inhomogeneities introduce additional scattering and attenuation. At the microscopic level, POFs are inherently heterogeneous due to the amorphous nature of polymeric materials. The structure consists of randomly coiled polymer chains, with radii of gyration typically on the order of hundreds of angstroms for high-molecular-weight polymers. This hierarchical organization gives rise to spatial fluctuations in density and composition. Material inhomogeneities may originate from polymer chain aggregation, dopant clustering, and density variations associated with physical aging processes such as enthalpy relaxation. Although such heterogeneity is intrinsic to amorphous polymers, its extent and spatial characteristics depend strongly on material composition, polymerization conditions, and thermal history during fiber fabrication. The refractive index can be engineered through controlled chemical modification and doping, enabling efficient light guidance. In parallel, the thermal and mechanical properties—closely linked to the underlying polymer structure—play a critical role in determining the fiber's stability and overall performance. In POFs, such fiber perturbations can be intentionally introduced through techniques such as bending, etching, corrugation, thermal treatment, or irradiation. Mode coupling plays a beneficial role by enhancing bandwidth and mitigating modal dispersion [13]. In practice, stronger mode mixing is often achieved using a mode scrambler positioned near the fiber input, which accelerates the redistribution of optical power among guided modes.

As light propagates along the fiber, the output field pattern gradually evolves from its initial launch condition. With sufficient propagation length, the system reaches a steady-state distribution (SSD), where all input conditions converge to a unique, characteristic far-field intensity profile. The fiber length required to achieve SSD defines the point at which the angular power distribution becomes independent of the launch conditions. Owing to its practical importance, mode coupling has been extensively investigated through different both theoretical and experimental approaches [14–20].

In this work, we extend the theoretical framework by formulating the stochastic mode coupling process using the Langevin equation. This approach enables a more comprehensive description of random perturbation effects and provides deeper insight into the statistical evolution of modal power distribution along multimode SI POFs.

2. The PFE and the Fokker–Planck Equation

Gloge's time-independent PFE is shown below [14]:

$$\frac{\partial P(\theta,z)}{\partial z} = -\alpha(\theta)P(\theta,z) + \frac{D}{\theta}\frac{\partial}{\partial \theta}\left(\theta\frac{\partial P(\theta,z)}{\partial \theta}\right) \quad (1)$$

where $P(\theta,z)$ is the angular power distribution, θ is the propagation angle to the core axis, z is the distance from the input end of the optical fiber, D is the constant coupling coefficient [14–18] and $\alpha(\theta)$ is the modal attenuation. Due to $\alpha(\theta)$ being negligible when $\theta \approx \theta_c$, Equation (1) becomes the following diffusion equation:

$$\frac{\partial P(\theta,z)}{\partial z} = \frac{D}{\theta}\frac{\partial P(\theta,z)}{\partial \theta} + D\frac{\partial^2 P(\theta,z)}{\partial \theta^2} \quad (2)$$

Accordingly, the internal redistribution of optical power in multimode fibers can be viewed as a diffusion-like process. It is well established that stochastic differential equations (SDEs) provide an effective framework for describing systems influenced by

random perturbations and are widely used to model diffusion phenomena [21]. Since mode coupling in multimode optical fibers originates from intrinsic randomness, it can be naturally described within an SDE-based formulation. In this context, Equation (2) can be approximated as follows:

$$\frac{\partial P(\theta,z)}{\partial z} = -V\frac{\partial P(\theta,z)}{\partial \theta} + D\,\frac{\partial^2 P(\theta,z)}{\partial \theta^2} \tag{3}$$

where V is assumed constant since the strength of mode coupling is θ-independent [14–16]. If we consider $P(\theta,z)$ as a probability distribution, Equation (3) is therefore revealed to be the Fokker–Planck equation with constant drift coefficient V and diffusion coefficient D [21]. The drift coefficient V is given as:

$$V = (1/M)\sum_{r=1}^{M} V_r \tag{4}$$

where V_r is the drift coefficient of the r-th mode. The process of determining the drift coefficient is illustrated in the next part.

3. The Langevin Equation

The Fokker–Planck Equation (3) is transformed into the following form of the Langevin equation [21]:

$$\frac{d\theta}{dz} = h + g\Gamma(z) \tag{5}$$

where $g\Gamma(z)$ is the Gaussian distributed random Langevin force with the strength g. This equation is also called SDE due to the fact that it contains the random force, such that we have [9]:

$$\begin{aligned} &\langle \Gamma(z) \rangle = 0 \\ &\langle \Gamma(z)\Gamma(z') \rangle = 2\delta(z-z') \end{aligned} \tag{6}$$

By adhering to the Ito rule [21], one gets $V = h$ and $D = g^2$. Hence, the drift and diffusion coefficients of the Fokker–Planck equation can be utilized to express the Langevin equation as follows:

$$\frac{d\theta}{dz} = V + \sqrt{D}\,\Gamma(z) \tag{7}$$

The first term on the right-hand side of Equation (7) represents a purely deterministic contribution, which drives the distribution toward $\theta = 0$. In contrast, the second term accounts for the stochastic nature of the system, reflecting the influence of intrinsic perturbations and internal noise within the fiber, and leads to a broadening of the angular (θ) distribution. It should be noted that, upon applying the boundary condition in Equation (7), the equation simplifies to Equation (8). Specifically, when the boundary condition from Equation (2), $D(\partial P/\partial\theta) = 0$ at $\theta = 0$, is satisfied, Equation (7) reduces to Equation (8):

$$\frac{d\theta}{dz} = \sqrt{D}\,\Gamma(z) \tag{8}$$

In order to integrate the Langevin Equation (7) from the input fiber end at $z = 0$ to some finite fiber length $z = z_f$, we first divide this length into N finite steps of length k, namely $k = z_f/N$. The angle θ_{n+1} at optical fiber length z_{n+1} could be calculated by solving the discretized Langevin Equation (7), which is re-written as:

$$\theta_{n+1} = \theta_n + Vk + \sqrt{Dk}\,\omega_n \tag{9}$$

where $n = 0, \ldots, N-1$ and $\omega_0, \ldots, \omega_{N-1}$ are independent Gaussian random numbers with zero mean and with variance 2, i.e., $< \omega_n >= 0$ and $< \omega_n \omega_{n'} >= 2\delta_{nm}$.

According to Equation (8), Equation (9) for $\theta_n = 0$ becomes:

$$\theta_{n+1} = \sqrt{Dk}\omega_n \tag{10}$$

Thus, the final angular value can be expressed as $\theta_N = \theta\left(z_f\right)$. By generating a large number of realizations of ω_n and averaging them over intervals $\Delta\theta$ within the range $0 \leq \theta \leq \theta_c$, the mean value $< \theta\left(z_f\right) >$ can be obtained (Figure 1). It is important to emphasize that perturbations in optical fibers are inherently random. Although the PFE (2) and the Fokker–Planck Equation (3) provide deterministic frameworks for describing energy redistribution, they do not fully account for the stochastic nature of mode coupling arising from these perturbations. In contrast, the Langevin equation explicitly incorporates random forces, enabling a more realistic and physically representative description of the underlying stochastic processes. Accordingly, this study employs the Langevin approach to analyze mode coupling and the resulting SSD in SI POFs.

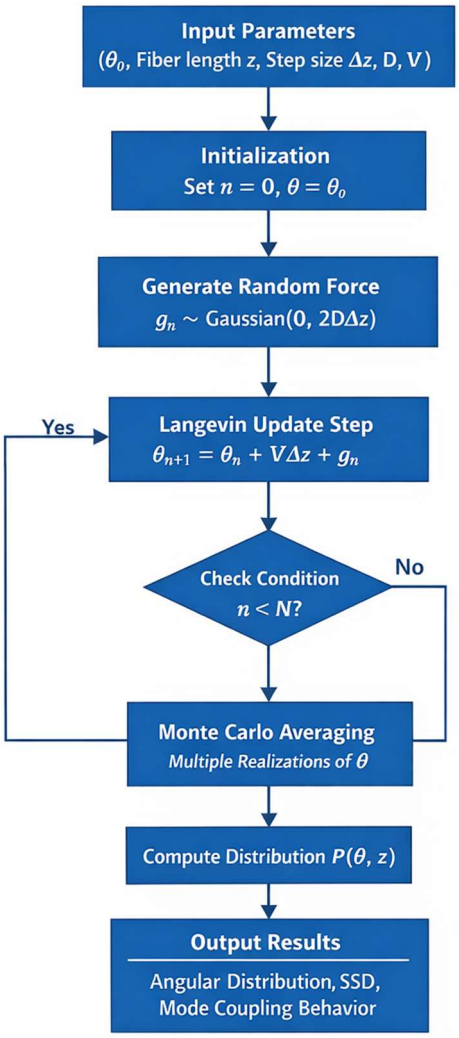


Figure 1. Block diagram of the Langevin equation solution for mode coupling, showing initialization, stochastic updates, Monte Carlo averaging, and computation of the angular distribution and steady-state behavior, where $\Delta z \equiv k$ and $g_n = \sqrt{D\Delta z}\,\omega_n$.

4. Numerical Results and Discussion

In this section we compare the numerical solution of the Langevin equation under a steady-state condition with our previously reported experimental data [22]. The SI POF investigated in this work has critical angle θ_c = 23.7° and coupling coefficient D = 2.4 × 10^{-4} rad^2/m [22]. With a constant step-length k = 0.0005 m, the Langevin equation is solved using Monte Carlo sampling of 5 × 10^5 representations of the ω_n in Equations (9) and (10) in the intervals of $\Delta\theta = 0.05°$. We present results for four different input angles $\theta_0 = 0,\ 6,\ 12$ and 16°. Figure 2 shows the normalized intensity distribution in the SI POF at different lengths for different launch angles θ_0 obtained as numerical solutions of the Langevin Equation (9). Radiation patterns in the short POF shown in Figure 2a reveal that distributions of low-order modes have shifted towards $\theta = 0°$. Longer POF lengths allow for the coupling of higher-order modes as shown in Figure 2b. When the transmission distance reaches z = 140 m (Figure 2d), the optical power distribution becomes independent on the launch conditions and does not vary with further increase in fiber length, indicating that an SSD is achieved. It should be noted that we have determined the drift coefficient $V = (-0.008 \pm 0.001)$ rad/m for the investigated SI POF by averaging drift coefficients $V_r (r = 1, 2, 3)$ for modes with launch angles $\theta_0 = 6,\ 12$ and 16° in Equation (4).

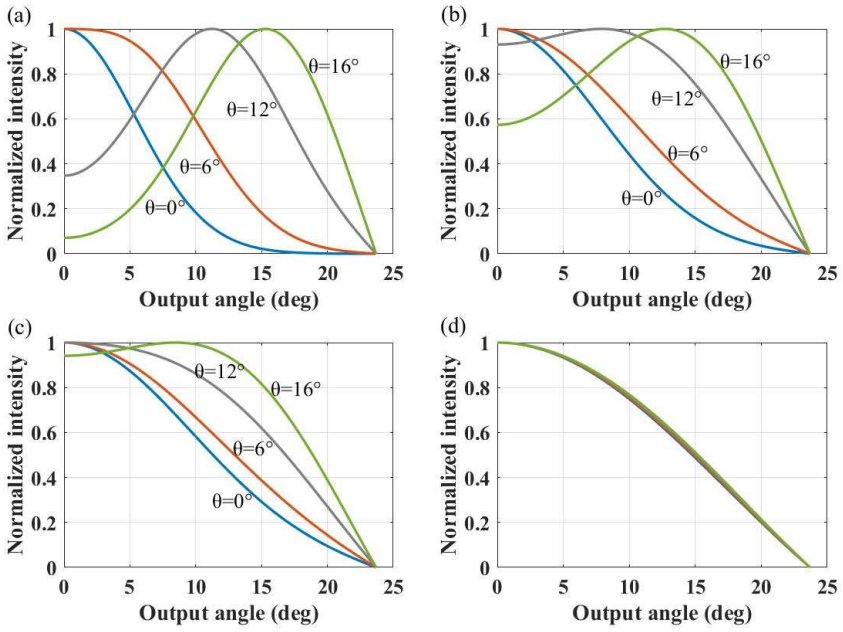


Figure 2. Normalized intensity distributions obtained as the numerical solution of the Langevin Equation (2) for SI POF at different transmission distances: (**a**) z = 10 m, (**b**) z = 30 m, (**c**) z = 50 m and (**d**) z = 140 m for different launch angles θ_0 = 0°, 6°, 12° and 16°.

Figure 3 compares SSD in the analyzed SI POF obtained as a numerical solution of the Langevin equation and experimental data [22]. One can observe a good match between the calculated and experimental data for the SSD. This length required to achieve SSD is much shorter than that typically observed shorter length for achieving SSD than that in silica optical fibers (SOFs), where SSD is usually reached over several kilometers. This difference can be attributed to the weaker intrinsic perturbation effects in the SOFs ($D \cong 10^{-7}$–10^{-6} rad^2/m) [23].

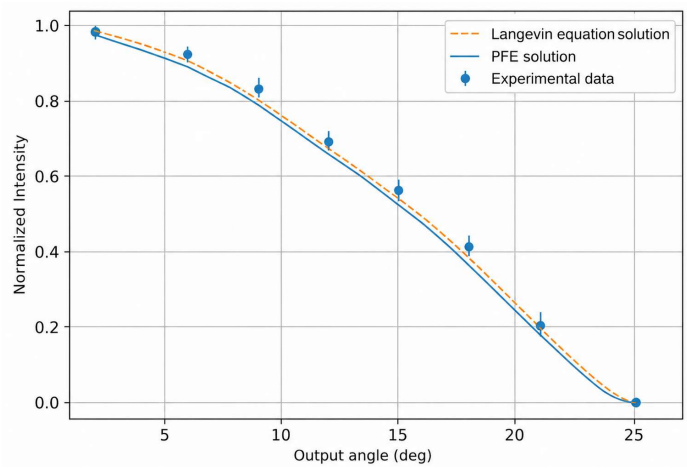


Figure 3. A comparison of SSD in the SI POF obtained as a numerical solution of the Langevin equation and PFE with experimental data [22], at fiber length z = 140 m.

Unlike the Fokker–Planck equation and the PFE, which require a very fine mesh in the finite difference approach to achieve high numerical accuracy (resulting in high memory consumption), the Langevin equation avoids this issue. The effectiveness of the Langevin equation integration algorithm and the explicit finite difference algorithm for solving the PFE can be evaluated in terms of time efficiency (execution speed) and algorithmic complexity. For the longest investigated fiber length of 140 m, the execution times on an Intel(R) Core(TM) i3 CPU 540 @ 3.07 GHz are t_{Lang} = 1.9 min for the Langevin equation and t_{PFE} = 2.5 min for the PFE. We calculated the speedup S between the Langevin equation approach and the finite difference method for solving the PFE, defined as $S = t_{PFE}/t_{Lang}$ = 1.32. The Langevin equation approach shows reduced sensitivity to variations in the coupling coefficient D and the launch angle, with these parameters varied over one order of magnitude. Therefore, the explicit finite difference solution of the PFE is considerably more complex and computationally intensive than the solution of the Langevin equation, which is consistent with the observed speedup and reduced parameter sensitivity.

In contrast to conventional deterministic coupled-power formulations, the present Langevin-based approach explicitly treats stochastic perturbations as intrinsic dynamical variables, enabling a direct statistical characterization of mode evolution and a more natural description of the observed steady-state distributions. Furthermore, the numerical solution of the Langevin equation exhibits significantly better agreement with the experimental data compared to the numerical solutions obtained using the PFE, highlighting the improved capability of the stochastic framework to capture the underlying physical behavior of the system.

In summary, we have demonstrated that the Langevin equation as a stochastic modeling framework can be effectively used to model mode coupling in multimode SI POFs [24,25]. Unlike the Fokker–Planck equation and the PFE, the numerical solutions of the Langevin equation are inherently stable and do not require special considerations. The results of this study can be applied to predict the signal transmission performance of SI POFs in communication and sensing systems.

5. Conclusions

In this paper, we analyzed mode coupling in multimode step-index polymer optical fibers (SI POFs) using the Langevin equation as a stochastic modeling framework. By incorporating numerically simulated Langevin forces, the approach enables accurate evaluation of modal power redistribution and steady-state distributions (SSDs) under realistic pertur-

bation conditions. The obtained numerical results show strong agreement with previously reported experimental data, confirming the validity of the model. From a telecommunications perspective, the proposed method provides an effective tool for characterizing modal dispersion, signal degradation, and bandwidth limitations in multimode SI POF links. This modeling framework supports improved design and optimization of short-reach optical communication systems, where SI POFs are increasingly deployed. Additionally, the results offer valuable insights for enhancing system reliability and performance in both data transmission and fiber-based sensing applications.

Author Contributions: Conceptualization, S.S. and M.S.; methodology, S.S., X.D., and M.S.; software, S.S. and M.S.; validation, X.D. and S.S.; visualization, S.S. and M.S.; writing—original draft preparation, M.S. and S.S.; writing—review and editing, S.S., M.S., and X.D.; supervision, S.S.; project administration, and funding acquisition, S.S. and X.D. All authors have read and agreed to the published version of the manuscript.

Funding: Funding for this study is provided by grants from the Serbian Ministry of Science, Technological Development, and Innovations (Agreement No. 451-03-34/2026-03/200122), and by grants from the National Natural Science Foundation of China (62001174) and the Sichuan Outstanding Youth Science and Technology Talents Project (2022JDJQ0047).

Data Availability Statement: The data presented in this study are available on request from the corresponding author.

Conflicts of Interest: The authors declare no conflicts of interest.

References

1. Puttnam, B.J.; Georg, R.; Ruben, L. Space-division multiplexing for optical fiber communications. *Optica* **2021**, *8*, 1186–1203. [CrossRef]
2. Min, R.; Liu, Z.; Pereira, L.; Yang, C.; Sui, Q.; Marques, C. Optical fiber sensing for marine environment and marine structural health monitoring: A review. *Opt. Laser Technol.* **2021**, *140*, 107082. [CrossRef]
3. Correa, C.R.B.; Huijskens, F.M.; Tangdiongga, E.; Koonen, A.M.J. Luminaire-free gigabits per second LiFi transmission employing WDM-over-POF. In Proceedings of the 46th European Conference on Optical Communications (ECOC), Brussels, Belgium, 6–10 December 2020; pp. 1–4.
4. Inoue, A.; Koike, Y. Unconventional plastic optical fiber design for very short multimode fiber link. *Opt. Express* **2019**, *27*, 12061–12069. [CrossRef] [PubMed]
5. Vázquez, C.; López-Cardona, J.D.; Montero, D.S.; Pérez, I.; Lallana, P.C.; Al-Zubaidi, F.M. Power over fiber in radio over fiber systems in 5G scenarios. In Proceedings of the 21st International Conference on Transparent Optical Networks (ICTON) 2019, Angers, France, 9–13 July 2019; pp. 1–4.
6. Al-Zubaidi, F.M.A.; Montero, D.S.; Vázquez, C. SI-POF supporting power-over-fiber in multi-Gbit/s transmission for in-home networks. *J. Light. Technol.* **2021**, *39*, 112–121. [CrossRef]
7. He, R.; Teng, C.; Kumar, S.; Marques, C.; Min, R. Polymer optical fiber liquid level sensor: A review. *IEEE Sens. J.* **2021**, *22*, 1081–1091. [CrossRef]
8. Wang, N.; Yao, Y.; Wu, P.; Zhao, L.; Chen, J. Soft polymer optical fiber sensors for intelligent recognition of elastomer deformations and wearable applications. *Sensors* **2024**, *24*, 2253. [CrossRef] [PubMed]
9. Huang, O.; Shi, J.; Chi, N. Performance and complexity study of a neural network post-equalizer in a 638-nm laser transmission system through over 100-m plastic optical fiber. *Opt. Eng.* **2022**, *61*, 126108. [CrossRef]
10. Apolo, J.A.; Ortega, B.; Almenar, V. Hybrid POF/VLC links based on a single LED for indoor communications. *Photonics* **2021**, *8*, 254. [CrossRef]
11. Fujimoto, D.; Lu, H.H.; Kumamoto, K.; Tsai, S.E.; Huang, Q.P.; Xie, J.Y. Phase-modulated hybrid high-speed Internet/WiFi/Pre-5G in-building networks over SMF and PCF with GI-POF/IVLLC transport. *IEEE Access* **2019**, *7*, 90620–90629. [CrossRef]
12. Sugihara, O. Gigabit and multi-gigabit data transmission for next-generation automotive optical network. In Proceedings of the 24th OptoElectronics and Communications Conference (OECC) 2019, Fukuoka, Japan, 7–11 July 2019; pp. 1–3.
13. Losada, M.Á.; Mazo, M.; López, A.; Muzás, C.; Mateo, J. Experimental assessment of the transmission performance of step index polymer optical fibers using a green laser diode. *Polymers* **2021**, *13*, 3397. [CrossRef] [PubMed]
14. Gloge, D. Optical power flow in multimode fibers. *Bell Syst. Tech. J.* **1972**, *51*, 1767–1783. [CrossRef]

15. Gambling, W.A.; Payne, D.N.; Matsumura, H. Mode conversion coefficients in optical fibers. *Appl. Opt.* **1975**, *14*, 1538–1542. [CrossRef] [PubMed]
16. Rousseau, M.; Jeunhomme, L. Numerical solution of the coupled-power equation in step index optical fibers. *IEEE Trans. Microw. Theory Tech.* **1977**, *25*, 577–585. [CrossRef]
17. Mateo, J.; Losada, M.A.; Garcés, I.; Zubia, J. Global characterization of optical power propagation in step-index plastic optical fibers. *Opt. Express* **2006**, *14*, 9028–9035. [CrossRef] [PubMed]
18. Savović, S.; Djordjevich, A. Influence of numerical aperture on mode coupling in step-index plastic optical fibers. *Appl. Opt.* **2004**, *43*, 5542–5546. [CrossRef] [PubMed]
19. Losada, M.A.; Mateo, J.; Garcés, I.; Zubía, J.; Casao, J.A.; Peréz-Vela, P. Analysis of strained plastic optical fibers. *IEEE Photon. Technol. Lett.* **2004**, *16*, 1513–1515. [CrossRef]
20. Muramoto, K.; Koike, Y. Ultra-low bit error rate plastic optical fiber link for high-speed PAM4 transmission: Enhanced optical return loss tolerance and alignment robustness. *Opt. Express* **2025**, *33*, 55120–55130. [CrossRef] [PubMed]
21. Risken, H. *The Fokker-Planck Equation*; Springer: Berlin/Heidelberg, Germany, 1989.
22. Dai, W.; Savović, S.; Zhao, C.; Shao, R.; Min, R. Theoretical and experimental investigation of the steady-state power distribution in multimode step-index plastic optical fibers. *Opt. Fiber Technol.* **2023**, *81*, 103531. [CrossRef]
23. Djordjevich, A.; Savović, S.; Tse, P.W.; Drljaca, B.; Simović, A. Mode coupling in strained and unstrained step-index glass optical fibers. *Appl. Opt.* **2010**, *49*, 5076–5080. [CrossRef] [PubMed]
24. Agrawal, G. *Nonlinear Fiber Optics*, 5th ed.; Academic Press: Oxford, UK, 2013.
25. Antonelli, C.; Mecozzi, A.; Shtaif, M.; Winzer, P.J. Random coupling between groups of degenerate fiber modes in mode multiplexed transmission. *Opt. Express* **2013**, *21*, 9484–9490. [CrossRef] [PubMed]

Disclaimer/Publisher's Note: The statements, opinions and data contained in all publications are solely those of the individual author(s) and contributor(s) and not of MDPI and/or the editor(s). MDPI and/or the editor(s) disclaim responsibility for any injury to people or property resulting from any ideas, methods, instructions or products referred to in the content.